Journal of Steroid Biochemistry & Molecular Biology 128 (2012) 76–86

Contents lists available at SciVerse ScienceDirect

Journal of Steroid Biochemistry and Molecular Biology

journal homepage: www.elsevier.com/locate/jsbmb

The role of residue C410 on activation of the human vitamin D receptor by various ligands

Hilda S. Castillo[a], Amanda M. Ousley[a], Anna Duraj-Thatte[a], Kelli N. Lindstrom[a], Dina D. Patel[c], Andreas S. Bommarius[b], Bahareh Azizi[a,*]

[a] School of Chemistry & Biochemistry, Parker H. Petit Institute for Bioengineering & Bioscience, Georgia Institute of Technology, Atlanta, GA 30332, USA
[b] School of Chemical & Biomolecular Engineering, Parker H. Petit Institute for Bioengineering & Bioscience, Georgia Institute of Technology, Atlanta, GA 30332, USA
[c] Emory University, Atlanta, GA 30322, USA

ARTICLE INFO

Article history:
Received 25 April 2011
Received in revised form 1 August 2011
Accepted 14 August 2011

Keywords:
Vitamin D receptor (VDR)
1α, 25-dihydroxyvitamin D_3 (1α, $25(OH)_2D_3$)
Lithocholic acid (LCA)
Cholecalciferol (chole)
Residue C410
Nuclear receptor

ABSTRACT

Nuclear receptors (NRs) are ligand-activated transcription factors that regulate the expression of genes involved in biologically important processes. The human vitamin D receptor (hVDR) is a member of the NR superfamily and is responsible for maintaining calcium and phosphate homeostasis. This receptor is activated by its natural ligand, 1α, 25-dihydroxyvitamin D_3 (1α, $25(OH)_2D_3$), as well as bile acids such as lithocholic acid (LCA). Disruption of molecular interactions between the hVDR and its natural ligand result in adverse diseases, such as rickets, making this receptor a good target for drug discovery. Previous mutational analyses of the hVDR have mainly focused on residues lining the receptor's ligand binding pocket (LBP) and techniques such as alanine scanning mutagenesis and site-directed mutagenesis. In this work, a rationally designed hVDR library using randomized codons at selected positions provides insight into the role of residue C410, particularly on activation of the receptor by various ligands. A variant, C410Y, was engineered to bind LCA with increased sensitivity (EC_{50} value of 3 μM and a 34-fold activation) in mammalian cell culture assays. Furthermore, this variant displayed activation with a novel small molecule, cholecalciferol (chole) which does not activate the wild-type receptor, with an EC_{50} value of 4 μM and a 25-fold activation. The presence of a bulky residue at this position, such as a tyrosine or phenylalanine, may contribute towards molecular interactions that allow for the enhanced activation with LCA and novel activation with chole. Additional bulk at the same end of the pocket, such as in the case of the variant H305F; C410Y enhances the receptor's sensitivity for these ligands further, perhaps due to the filling of a cavity. The effects of residue C410 on specificity and activation with the different ligands studied were unforeseen, as this residue does not line the hVDR's LBP. Further investigating of the structure–function relationships between the hVDR and its ligands, including the mutational tolerance of residues within as well as outside the LBP, is needed for a comprehensive understanding of the functionality and interactions of the receptor with these ligands and for development of new small molecules as potential therapeutic drugs.

© 2011 Elsevier Ltd. All rights reserved.

1. Introduction

Nuclear receptors (NRs) are a large family of ligand-activated transcription factors, present in a number of organisms, including worms, insects, and humans [1]. To date, 49 members have been identified in the NR superfamily in humans [2,3]. These receptors have been shown to bind a variety of ligands, ranging from steroids to fatty acids and xenobiotic metabolites. Upon binding of a small molecule ligand, NRs function as transcription regulators of essential genes involved in physiological activities, such as development, growth, and homeostasis [4–6]. These small molecules serve either as agonists, inducing transcription, or as antagonists, repressing transcription [7].

Due to their roles in a complex cascade of biological processes, the transcriptional regulation of NRs involves a series of molecular events. In the unliganded (*apo*) form or in the presence of an antagonist, most NRs associate with corepressors which form protein complexes comprising of histone deacetylases (HDACs), causing the condensation of chromatin over target promoter regions [8,9]. Hence, gene expression is repressed. Upon binding of a small hydrophobic molecule (*holo*-form), such as an agonist, a

* Corresponding author at: School of Chemistry & Biochemistry, Georgia Institute of Technology, 901 Atlantic Drive, Atlanta, GA 30332, USA. Tel.: +1 404 894 6077; fax: +1 404 894 2295.
E-mail addresses: hilda.castillo@chemistry.gatech.edu (H.S. Castillo), gth783d@mail.gatech.edu (A.M. Ousley), annaduraj@gatech.edu (A. Duraj-Thatte), klindstrom3@gatech.edu (K.N. Lindstrom), ddpate2@emory.edu (D.D. Patel), andreas.bommarius@chbe.gatech.edu (A.S. Bommarius), bahareh.azizi@chemistry.gatech.edu (B. Azizi).

0960-0760/$ – see front matter © 2011 Elsevier Ltd. All rights reserved.
doi:10.1016/j.jsbmb.2011.08.003

conformational change occurs leading to the association of these receptors with coactivator protein complexes comprising of histone acetyltransferases (HATs) [8,10–12]. These proteins modify the chromatin structure over target promoter regions such that the recruitment of general transcription machinery including RNA polymerase is facilitated, resulting in gene activation.

Despite their ability to control a wide variety of processes, NRs share highly conserved sequences and modular protein structures that consist of several domains, with particular emphasis focused on the DNA binding domain (DBD) and ligand binding domain (LBD) [3,13]. The DBD which consists of zinc-finger motifs is the most conserved domain among NRs, and is responsible for binding specific DNA sequences called response elements (REs) [14,15]. The LBD's overall structure is moderately conserved, sharing a common three-dimensional structure mostly composed of α-helices and a few β-strands, arranged in an 'α-helical sandwich' [16]. Within this sandwich is a predominantly hydrophobic ligand binding pocket (LBP), whose residues are involved in primary interactions with the ligand, providing a level of diversity among the various NRs. One important feature of the LBD is the terminal helix, helix 12 in most NRs, which contains the ligand dependent activation function domain (AF-2). The previously mentioned conformational change that is essential to the activation of these receptors is drastically observed in this helix, which forms a mobile lid over the LBP upon agonist binding [17]. As part of its function, this domain is also involved in receptor dimerization and coregulator interactions [18–21].

As an endocrine member of the NR superfamily, the 427-amino acid long human vitamin D receptor (hVDR) plays a major role in maintaining calcium and phosphate homeostasis, as well as regulating bone metabolism [22,23]. Furthermore, this receptor is involved in anti-proliferative, pro-apoptotic and immunosuppressive activities [24]. Mutations in the hVDR have been shown to disrupt receptor interactions leading to insufficient receptor function; thus resulting in adverse consequences or diseases, such as rickets [25–27]. The receptor's LBD consists of 303 amino acids and forms the canonical 'α-helical sandwich', while the elongated LBP is 697 $Å^3$ with the natural ligand occupying 56% of this volume [16,26]. Ligands of the hVDR include the natural ligand, 1α, 25-dihydroxyvitamin D_3 (1α, 25$(OH)_2D_3$), as well as bile acids such as lithocholic acid (LCA) (Fig. 1a) [28]. Molecular interactions between the hVDR and 1α, 25$(OH)_2D_3$ involve both hydrophobic and electrostatic interactions that are crucial for the activation and function of the receptor, with residues Y143, S237, R274, S278, H305 and H397, for example, forming important hydrogen bonds (Fig. 1b) [26].

Investigating the structure–function relationships between the hVDR and its ligands is of interest, specifically for further understanding of the functionality of the receptor, its ability to bind various ligands, and for development of new small molecules as therapeutic drugs. Previous mutational analyses of the hVDR have focused on alanine scanning mutagenesis and site-directed mutagenesis of the residues lining the LBP of the receptor [29–33]. A study on the hVDR residues that form hydrogen bonds with the natural ligand showed that in general, mutations had a greater effect on activation than binding [34]. This work also suggested that maintaining proper residue packing could be more important than maintaining hydrogen bonding interactions. Additionally, the recently solved crystal structure of the hVDR with 1α, 25$(OH)_2$-3-epi-D_3 has provided insight on the role of water in maintaining hydrogen bonding interactions similar to those of the natural ligand [35]. These studies and others have provided a fundamental understanding of the key interactions between the hVDR and various ligands, however work on the mutational tolerance of LBP residues or the effects of residues outside the LBP has been limited [36–41]. Therefore, the focus of this work was to further investigate the structural and functional parameters of the hVDR, through engineering of this receptor to bind and activate in response to a novel small molecule, cholecalciferol (chole). Chole, a precursor in the 1α, 25$(OH)_2D_3$ biosynthetic pathway lacks two of the three hydroxyl groups present in 1α, 25$(OH)_2D_3$ and does not activate the hVDR, confirming the importance of precise molecular interactions required for ligand activation (Fig. 1a). By using chole as a target ligand, the receptor's hydrogen bonding capabilities are limited to one hydroxyl group, perhaps allowing for a further assessment on the importance of hydrogen bonding for the stability and function of the receptor (Fig. 1).

2. Materials and methods

2.1. Ligands

1α, 25-dihydroxyvitamin D_3, lithocholic acid and cholecalciferol were purchased from BIOMOL (Plymouth Meeting, PA), MP Biomedicals, LLC (Solon, OH) and Sigma–Aldrich (St. Louis, MO), respectively. A 10 μM stock of 1α, 25-dihydroxyvitamin D_3 and 10 mM stocks of lithocholic acid and cholecalciferol, were made with 80% ethanol: 20% DMSO and stored at 4 °C.

2.2. hVDR gene isolation and construction of a yeast expression plasmid

The human vitamin D receptor gene was isolated and amplified from human skin cDNA (BioChain, Hayward, CA) via PCR using the following primers: 5′-gcc gga att cat gga ggc aat ggc ggc-3′ and 5′-gga cta gtt cag gag atc tca ttg cca aac ac-3′ (Operon, Huntsville, AL). The underlined sequences denote *EcoRI* and *SpeI* restriction sites, respectively. The hVDR gene and yeast expression plasmid pGBT9, which contains the Gal4 DBD, were digested with *EcoRI* and *SpeI*, ligated, and transformed into Z-competent™ XL-1 Blue *E. coli* cells (Zymo, Orange, CA). The resulting plasmid, pGBDhVDR, contained the Gal4 DBD fused to the full-length hVDR, and a tryptophan marker. All DNA was purified using the QIAprep® Spin Miniprep Kit (Qiagen, Valencia, CA). The pGBDhVDR plasmid was sequenced for confirmation (Operon, Huntsville, AL).

2.3. Creating a rationally designed hVDR library

The hVDR insert cassette variants were constructed using eight oligonucleotides containing randomized degenerate codons at the designated mutation sites. The synthetic oligonucleotides were designed to have overlapping complementary ends, forming a full insert cassette via a combination of hybridization and PCR [42]. The full insert cassette (1014 bp) was created using 100 ng of each oligonucleotide and 125 ng of the corresponding forward and reverse primers (Operon, Huntsville, AL) with the following thermocycler conditions: 95 °C 1 min, 59 °C 1 min, 72 °C 2 min, repeat 20 cycles, 95 °C 1 min, 56.6 °C 1 min, 72 °C 2 min, repeat 20 cycles, 72 °C 3 min. The full insert cassette was purified using the QIAprep® Spin Miniprep Kit (Qiagen, Valencia, CA).

A hVDR background plasmid was constructed to decrease the expression of the wild-type hVDR in the designed library. *SacII* and *KpnI* restriction sites were introduced into the pGBDhVDR yeast expression plasmid towards the beginning and end of the hVDR gene, respectively, via site-directed mutagenesis (Stratagene, Santa Clara, CA) to create the pGBDhVDRSacIIKpnI plasmid. This plasmid was digested with *SacII* and *KpnI*, removing 810 bp of the wild-type hVDR gene. A 145 bp segment of random DNA ('junk') from a pMSCVeGFP plasmid was amplified via PCR, digested and ligated between the *SacII* and *KpnI* sites in the pGBDhVDRSacIIKpnI plasmid. The ligation was transformed into Z-competent™ XL-1 Blue *E. coli* cells (Zymo, Orange, CA). When expression of the resulting

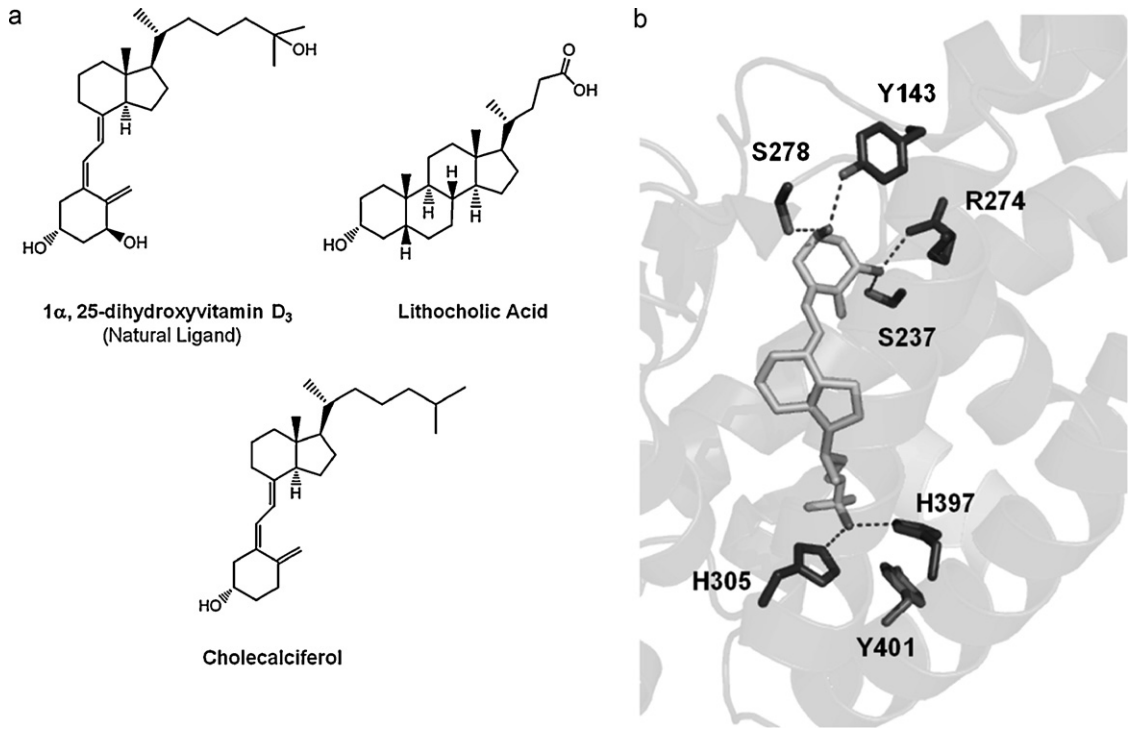

Fig. 1. (a) Structures of hVDR ligands and precursors. 1α, 25-dihydroxyvitamin D_3 (1α, 25$(OH)_2D_3$) and lithocholic acid (LCA) are known hVDR ligands. Cholecalciferol (chole) is a precursor in the 1α, 25$(OH)_2D_3$ biosynthetic pathway, lacking two of the three hydroxyl groups present in 1α, 25$(OH)_2D_3$. This molecule does not activate the hVDR. (b) Important hydrogen bonds between the hVDR and its natural ligand, 1α, 25$(OH)_2D_3$ (pdb: 1DB1). Bonds represented by (---). Residue Y401 which was targeted for mutagenesis in the rationally designed library, along with residue H397, is also shown.

plasmid, pGBDhVDRBackground, takes place three STOP codons are translated, resulting in a non-functional protein. All DNA was purified using the QIAprep® Spin Miniprep Kit (Qiagen, Valencia, CA). The pGBDhVDRBackground plasmid was sequenced for confirmation (Operon, Huntsville, AL).

2.4. Yeast transformation using the PJ69-4A strain

Using the 1× TRAFCO yeast transformation protocol, 1 μg of the full insert cassette and 0.3 μg of the yeast expression plasmids, pGBDhVDRBackground (containing a tryptophan marker, digested) and pGAD10BAACTR (containing the Gal4 activation domain fused to the ACTR human coactivator, and a leucine marker), were transformed into the PJ69-4A yeast strain [43]. Transformants were plated onto synthetic complete agar plates lacking leucine and tryptophan (SC-LW), as well as synthetic complete agar plates lacking adenine or histidine, leucine and tryptophan (SC-ALW or SC-HLW with 0.1 mM 3-AT) with 10 μM of various ligands. Plates were incubated at 30 °C for 3–4 days. A library size of $\sim 1.6 \times 10^3$ variants with a transformation efficiency of $\sim 2.9 \times 10^4$ cfu/μg DNA was achieved.

2.5. Liquid quantitation assays of chemical complementation in yeast

Variants obtained from the yeast transformation were grown overnight in non-selective media (SC-LW), at 30 °C with shaking at 300 rpm. A 4:1 ratio of selective media (SC-HLW with 0.1 mM 3-AT) with and without ligand at varying concentrations: cells (yeast resuspended in water) were aliquoted into 96-well plates. Plates were then incubated at 30 °C with shaking at 170 rpm for 48 h, with optical density readings at a wavelength of 630 nm (OD630) taken at 0, 24 and 48 h. All data points represent the mean of at least duplicate experiments and the bars indicate standard deviation. EC_{50} values were calculated using GraphPad Prism and a non-linear regression extrapolation.

2.6. Site-directed mutagenesis

Mutations were introduced into the yeast expression plasmid, pGBDhVDR, using PCR (Stratagene, Santa Clara, CA) and the corresponding mutagenic primers (Operon, Huntsville, AL). All plasmids were purified using the QIAprep® Spin Miniprep Kit (Qiagen, Valencia, CA) and sequenced for confirmation (Operon, Huntsville, AL).

2.7. Construction of mammalian expression plasmids

The Gal4 DBD fused to full-length hVDR (GBDhVDR) as well as each of the hVDR variants; C410Y, H305F, H397Y, H305F;H397Y, H305F;C410Y, H397Y;C410Y, and H305F;H397Y;C410Y, was amplified from the respective pGBD yeast expression plasmid via PCR using 125 ng of the following primers: 5′-tcc ccg cgg atg aag cta ctg tct tct atc gaa caa g-3′ and 5′-aag gaa aaa agc ggc cgc tca gga gat ctc att gcc aaa ca-3′ (Operon, Huntsville, AL). The underlined sequences denote *SacII* and *NotI* restriction sites, respectively. The fusion constructs and mammalian expression plasmid pCMX, which contains a cytomegalovirus (CMV) promoter, were digested with *SacII* and *NotI*, ligated, and transformed into Z-competent™ XL-1 Blue *E. coli* cells (Zymo, Orange, CA). The resulting plasmids, pCMXGRhVDR, pCMXGRhVDRC410Y, pCMXGRhVDRH305F, pCMXGRhVDRH397Y, pCMXGRhVDRH305F;H397Y, pCMXGRhVDRH305F;C410Y, pCMXGRhVDRH397Y;C410Y, and pCMXGRhVDRH305F;H397Y;C410Y were purified using the QIAprep® Spin Miniprep Kit (Qiagen, Valencia, CA) and sequenced for confirmation (Operon, Huntsville, AL).

2.8. Mammalian cell culture assays

Human embryonic kidney 293T cells (HEK 293T, ATCC, USA) were transfected with the pCMX mammalian expression plasmids discussed above, along with the p17*4TATAluc and pCMXβ-gal reporter plasmids as described by Taylor et al., using Lipofectamine 2000 (Invitrogen, Carlsbad, CA) as the cationic lipid [44]. p17*4TATAluc contains the *Renilla* luciferase gene under the control of four Gal4 REs located upstream of a minimal thymidine kinase promoter, while pCMXβ-gal contains the β-galactosidase gene under the control of the mammalian CMV promoter. Cells were harvested ~36–48 h after the addition of ligand at varying concentrations, and analyzed for luciferase and β-galactosidase activity. All data points represent the mean of triplicate experiments normalized against β-galactosidase activity and the bars indicate standard deviation. EC_{50} values were calculated using GraphPad Prism and a non-linear regression extrapolation. Fold activations were calculated by dividing the highest level of activation by the lowest level of activation in triplicate experiments.

2.9. In silico docking of wild-type hVDR and hVDRC410Y with cholecalciferol

The structure of the hVDRC410Y variant was prepared *in silico* using the program TRITON 4.0.0 (National Centre for Biomolecular Research, Czech Republic) and its external program MODELER (National Centre for Biomolecular Research, Czech Republic). A computational site-directed mutagenesis method, where the wild-type protein is used for homology modeling was employed [45,46]. The atomic coordinates of the crystal structure of the hVDR ligand binding domain (Δ165–215) were retrieved from the research collaboratory for structural bioinformatics (RCSB) protein data bank (PDB) (PDB ID: 1DB1) [26,47].

The wild-type hVDR and hVDRC410Y structures were prepared for docking using the UCSF CHIMERA-interactive molecular graphics program by: (1) removing the ligand and water molecules, (2) adding polar hydrogens, and (3) assigning Gasteiger charges [48]. The three-dimensional structure of cholecalciferol was constructed and minimized using ChemBioDraw Ultra 11.0 and ChemBio3D Ultra 11.0 (Cambridge Soft, USA) [49]. AutoDockTools was used to add Gasteiger charges, setting the partial charge property of each ligand atom. Docking simulations were performed using AutoDock Vina with default parameters, such that the protein was held rigid and the ligand was allowed free rotation [50]. The receptor–ligand poses of lowest free energy of binding were analyzed further using the PyMOL molecular graphics system (DeLano Scientific LLC, USA).

3. Results

3.1. Chemical complementation: a genetic selection system in yeast

The function of the wild-type hVDR and the variants obtained from the hVDR library discussed in this work was assessed in a genetic selection system in yeast called chemical complementation (CC). In CC the survival of yeast, *Saccharomyces cerevisiae*, is linked to the binding and activation of a NR by a small molecule ligand. The activation of the NR results in the transcription of an essential gene, allowing CC to serve as a powerful tool for engineering nuclear receptors [44,51–55]. CC involves the use of the yeast strain, PJ69-4A, which contains Gal4 REs controlling the expression of the selection markers, *HIS*3 and *ADE*2 [56]. In CC, the Gal4 DBD is fused to a NR LBD, the Gal4 activation domain (AD) is fused to a human coactivator, and a small molecule ligand is introduced (Fig. 2a) [51,52]. Upon ligand binding, the Gal4 AD:coactivator fusion protein associates with the NR LBD, leading to transcription of the *HIS3 or ADE2* selective gene. Thus yeast survive on media lacking the essential nutrient but containing the small molecule ligand. Overall, CC provides simple and rapid detection of NR activation, making this selection system useful for semi high-throughput evaluations of receptor–ligand interactions [51,52,57].

To determine the activity of the wild-type hVDR in the chemical complementation system in yeast, the hVDR gene was isolated and amplified from skin cDNA and cloned into a yeast expression plasmid containing the Gal4 DBD. This construct (pGBDhVDR) along with another yeast expression plasmid, containing the Gal4 AD fused to the ACTR (activator for thyroid and retinoid receptors) human coactivator (pGAD10BAACTR), were tested in liquid quantitation assays of chemical complementation with 1α, $25(OH)_2D_3$, LCA and chole in histidine selective media. The *HIS3* gene encodes imidazoleglycerol-phosphate dehydratase, an essential enzyme in the histidine biosynthetic pathway [58]. Due to the known 'leaky expression' of the *HIS3* gene, 3-amino-1, 2, 4-triazole (3-AT), an inhibitor of imidazoleglycerol-phosphate dehydratase (*HIS3* protein), was used to reduce basal growth. Gal4 is a ligand independent transcription factor used as a positive control, and as expected displayed growth independent of the presence of ligand (Fig. 2b and c). As shown in Fig. 2b, ligand activated growth at 1 nM with an $EC_{50} = 2$ nM (based on growth) was observed for the wild-type hVDR with 1α, $25(OH)_2D_3$ in histidine selective media (SC-HLW with 0.1 mM 3-AT). Ligand activated growth was also observed with LCA at 10 μM, for which the wild-type hVDR displayed an $\sim EC_{50} > 10$ μM, as shown in Fig. 2c. Growth was not observed with chole as expected, as this molecule is an inactive precursor in the 1α, $25(OH)_2D_3$ biosynthetic pathway (Fig. 2c). Since the EC_{50} values obtained in chemical complementation with the Gal4 DBD:hVDR fusion protein correlated to previously reported cell culture data, CC proved to be a suitable system for evaluating hVDR variants with various ligands [59,60].

3.2. Rational design and construction of a hVDR library

A rational mutagenic approach was used to engineer the hVDR to bind and activate in response to chole, while investigating the tolerance level of residues in the receptor's LBP for amino acids of varying chemical and physical properties, such as volume and hydrophobicity. The crystal structure of the hVDR with 1α, $25(OH)_2D_3$ (PDB:1DB1) was analyzed using Visual Molecular Dynamics (VMD), a molecular graphics software program [26,61]. Residues within five angstroms of the ligand, as well as key molecular interactions in the hVDR's LBP (e.g. hydrogen bonds and Van der Waals interactions) were determined. Using previous mutational analyses, specific residues that interact directly with 1α, $25(OH)_2D_3$ and/or are predicted to have an effect on stabilizing the active conformation of the receptor were chosen as target residues [29–33]. Based on these analyses, two residues were targeted for mutagenesis in the discussed library, H397 and Y401.

H397 was chosen due to its known important hydrogen bond with the 25-hydroxyl group of 1α, $25(OH)_2D_3$, contributing to the position of helix 11 and the folding of the receptor into its active conformation [26,29–33]. However, chole lacks this hydroxyl group on the aliphatic chain and therefore cannot form the hydrogen bond that 1α, $25(OH)_2D_3$ forms with this residue. This generated interest in the mutational tolerance at this residue, as well as, in determining whether the receptor would maintain hydrogen-bonding capability at this position even though the target molecule lacks a functional group that would contribute to this interaction. Y401, on the other hand, shares a

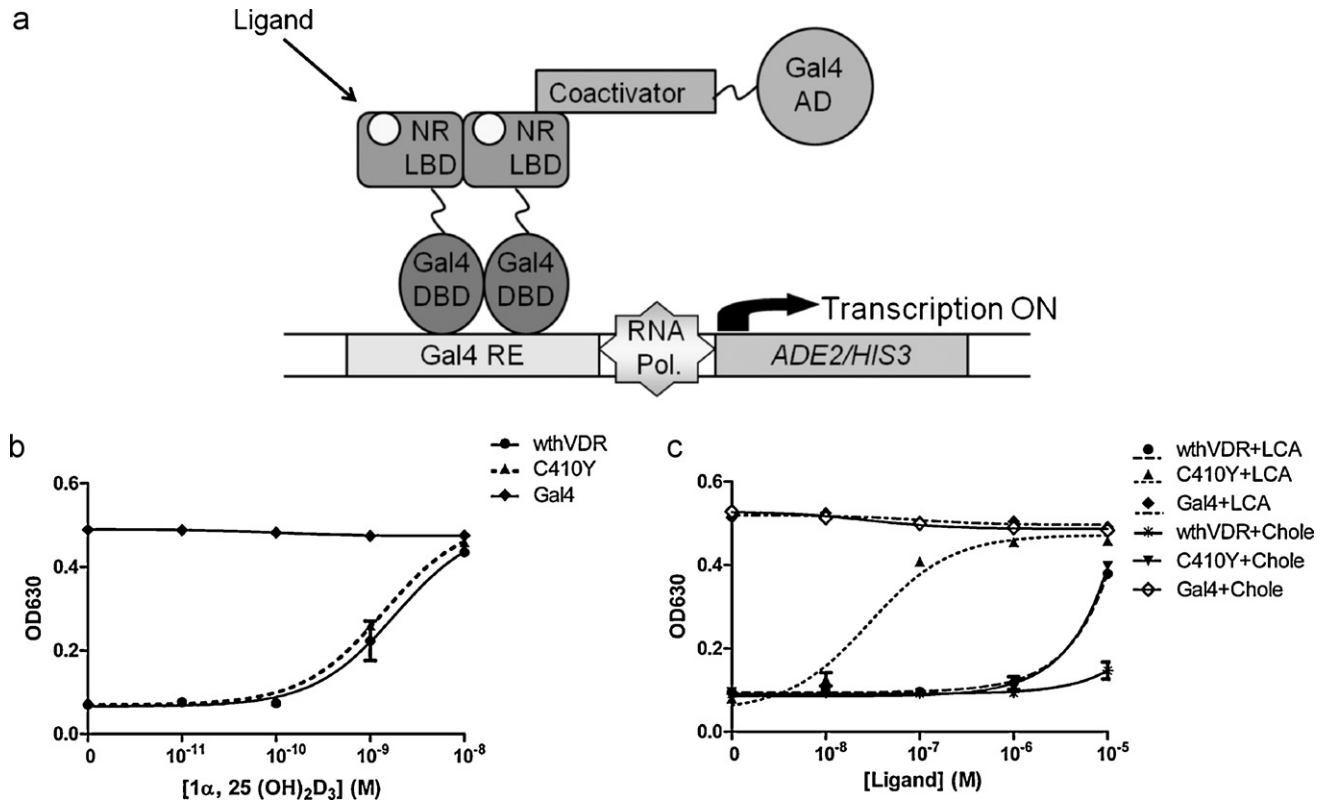

Fig. 2. (a) Chemical complementation (CC) genetic selection assay in yeast. CC is a genetic selection system, in which the survival of yeast is linked to the activation of a nuclear receptor (NR) by a small molecule ligand. The PJ69-4A yeast strain contains the genetic selection genes *HIS*3 and *ADE*2 under the control of Gal4 response elements (REs). In this system, the Gal4 DNA binding domain (DBD):NR ligand binding domain (LBD) fusion protein binds Gal4 REs and an agonist binds the NR LBD leading to the recruitment of the corresponding Gal4 activation domain (AD):coactivator fusion protein and the transcriptional machinery. Thus resulting in the expression of the *HIS3* or *ADE2* gene. Transcription of the regulated gene allows the yeast strain to produce its own histidine or adenine and survive on media lacking that nutrient. Therefore, only ligand activated NRs will result in the survival of yeast. Quantitation assays of wthVDR and hVDRC410Y in histidine selective media with (b) 1α, 25(OH)2D3. Ligand activated growth is observed for wild-type hVDR and C410Y at 1 nM. (c) LCA and chole. Ligand activated growth is observed for wild-type hVDR at 10 μM LCA, however growth is not observed with chole. Ligand activated growth is observed for C410Y at 100 nM LCA and 10 μM chole. Gal4 is a ligand independent transcription factor and was used as a positive control. Optical density readings were taken at a wavelength of 630 nm (OD630), measuring cell growth based on turbidity.

hydrophobic interaction with helix 12 and contributes to the folding of the AF-2 surface [26,29–33]. Due to the role this residue plays in mediating receptor–coactivator/corepressor interactions with the natural ligand, interest was generated in determining the tolerance of this residue for other amino acids when the target molecule, in this case chole, is smaller in volume compared to 1α, 25(OH)$_2$D$_3$. Mutations at each of the two residues targeted for mutagenesis were designed based on amino acid properties (e.g. polarity, shape and volume), sequencing alignments of the hVDR with other NRs, and evolutionarily conserved and non-conserved residues [38,62].

The library of hVDR variants was constructed using oligonucleotides with randomized degenerate codons at residues H397 and Y401. These oligonucleotides also contained overlapping complementary ends with the former and latter oligonucleotide in sequence, thus a full insert cassette was created via a combination of hybridization and PCR [42]. The ends of the full insert cassette also contained complementary sequences to a plasmid containing the Gal4 DBD. Once transformed into the PJ69-4A yeast strain, through homologous recombination, the insert cassettes and the Gal4 DBD plasmid generate yeast expression vectors containing hVDR variants fused to the Gal4 DBD. Colonies from selective plates containing ligand were tested in liquid quantitation assays of chemical complementation.

3.3. Variant hVDRC410Y in yeast and mammalian cell culture assays

A variant containing an undesigned mutation at the C410 position to a tyrosine (C410Y) was discovered, and exhibited a ligand activated growth profile similar to that of the wild-type hVDR with 1α, 25(OH)$_2$D$_3$, with growth at 1 nM and an EC$_{50}$ ≈ 2 nM, in histidine selective media (SC-HLW with 0.1 mM 3-AT) (Fig. 2b). As shown in Fig. 2c the variant displayed ligand activated growth with LCA, with growth at 100 nM and an EC$_{50}$ = 29 nM, drastically showing approximately a 100-fold increase in sensitivity compared to the wild-type receptor. Furthermore, this variant showed ligand activated growth with a novel small molecule, cholecalciferol (chole), in the same media at 10 μM with an ~EC$_{50}$ > 10 μM (Fig. 2c).

To determine whether the C410Y results obtained in yeast with chemical complementation were consistent with mammalian cell culture assays, the variant and wild-type hVDR (fused to the Gal4 DBD) were cloned into a mammalian expression plasmid containing a cytomegalovirus (CMV) promoter. Human embryonic kidney cells (HEK 293T) were transfected with the receptor and a reporter plasmid containing the *Renilla* luciferase gene under the control of four Gal4 REs (p17*4TATAluc), and tested with 1α, 25(OH)$_2$D$_3$, LCA and chole. As shown in Fig. 3a the wild-type hVDR and C410Y showed similar activation profiles with 1α, 25(OH)$_2$D$_3$, displaying EC$_{50}$ values of 5 nM and 1 nM, and 198- and 76-fold activations,

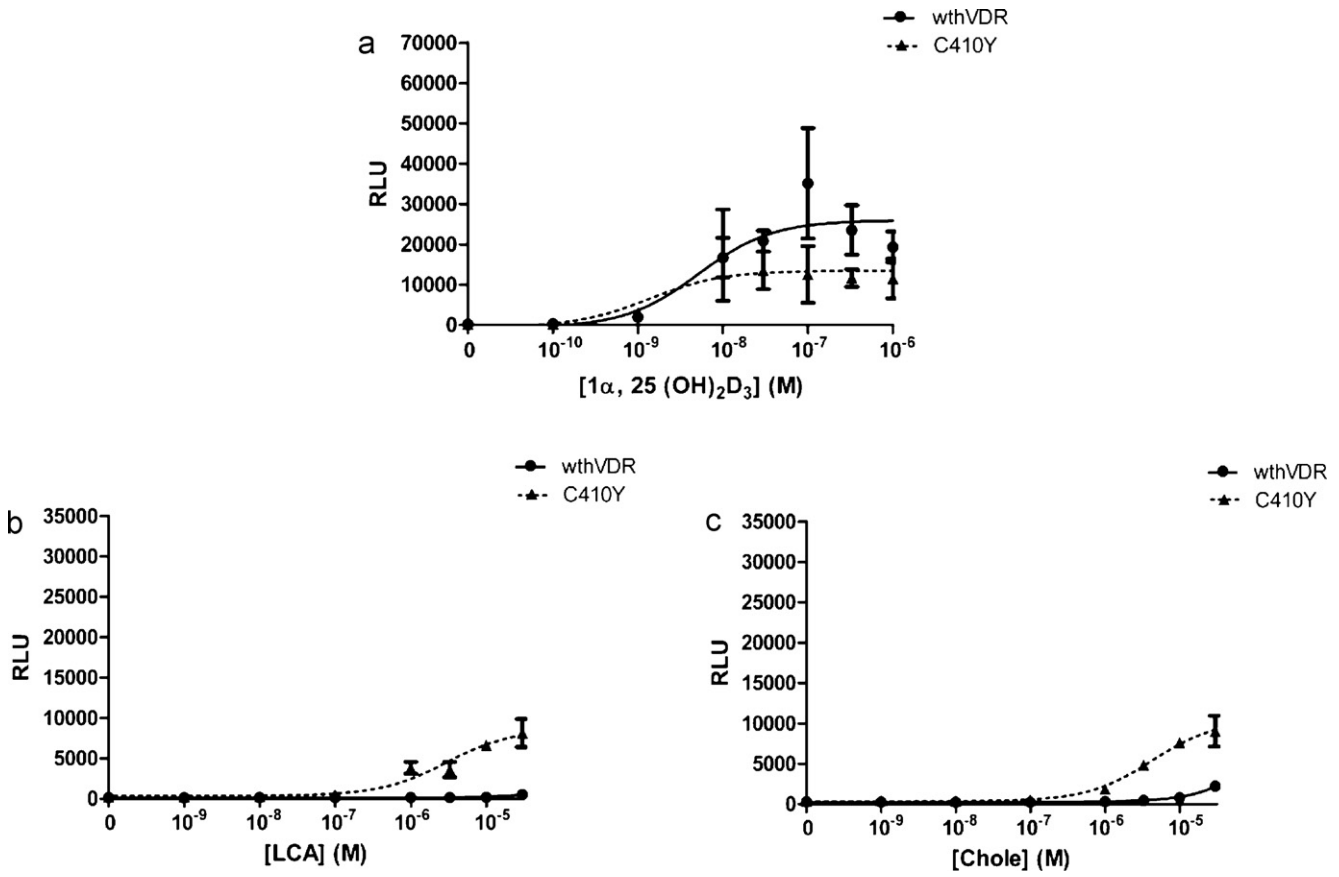

Fig. 3. Variant hVDRC410Y is activated by a novel small molecule: activity of wthVDR and hVDRC410Y in mammalian cell culture assays using human embryonic kidney cells (HEK 293T) with (a) 1α, 25$(OH)_2D_3$ (b) LCA and (c) chole. A hVDR variant, C410Y, activated by LCA with enhanced sensitivity in comparison to the wild-type hVDR, and that is also activated by the novel small molecule, cholecalciferol, was engineered. Activity was measured in relative light units (RLU) derived from the measurement of luciferase activity and normalized against β-galactosidase activity. See Table 1 for EC_{50}, fold activation and maximum activation values.

respectively (Table 1). As expected, C410Y showed an EC_{50} value of 3 μM and a 34-fold activation with LCA, displaying approximately a 100-fold increase in sensitivity compared to the wild-type receptor which has previously been shown to display activation at 100 μM (Fig. 3b and Table 1). Consistent with results from chemical complementation and as shown in Fig. 3c, C410Y showed an EC_{50} value of 4 μM and a 25-fold activation with chole (Table 1).

3.4. Mutational tolerance of residue C410 in the hVDR

Naturally, the fact that residue C410 was not targeted in the designed library and that the mutation C410Y resulted in a unique activation profile with both LCA and chole led to further investigation of this position. The C410 residue is located in the loop between helices 11 and 12 of the hVDR's LBD and is not known to make any direct contacts with the natural ligand (approximately eight angstroms from the 25-hydroxyl group of 1α, 25$(OH)_2D_3$) (Fig. 4a) [26]. To determine whether the enhanced C410Y activity was specifically due to the presence of a tyrosine or whether another amino acid would display similar activation profiles to those of the C410Y variant, this residue was mutated to amino acids of varying polarity, shape and volume (e.g. phenylalanine, alanine, serine, asparagine, tryptophan, histidine, leucine, methionine, threonine and lysine) via site-directed mutagenesis. Although supported by previous work, such as that of Carlberg, Ishizuka, and Mizwicki, drastic changes in the activation profiles of the resulting

Table 1
EC_{50}, fold activation and maximum activation values for the hVDR constructs in mammalian cell culture assays using HEK 293T cells with 1α, 25$(OH)_2D_3$, LCA and chole.

hVDR construct	1α, 25$(OH)_2D_3$			LCA			Chole		
	EC_{50}	Fold activation	Maximum activation (RLU)	EC_{50}	Fold activation	Maximum activation (RLU)	EC_{50}	Fold activation	Maximum activation (RLU)
wthVDR	5 nM	198 ± 83	35,139	>32 μM	<10	539	>32 μM	<10	2241
C410Y	1 nM	76 ± 57	17,311	3 μM	34 ± 7	8138	4 μM	25 ± 5	9043
H305F	4 nM	135 ± 30	39,406	~10 μM	103 ± 22	22,955	2 μM	98 ± 31	20,494
H397Y	9 nM	201 ± 88	21,540	>32 μM	<10	177	>32 μM	<10	488
H305F;H397Y	4 nM	75 ± 31	16,934	~10 μM	38 ± 3	9629	0.3 μM	42 ± 9	12,268
H305F;C410Y	<1 nM	54 ± 25	20,513	0.3 μM	28 ± 13	10,801	0.2 μM	14 ± 12	5846
H397Y;C410Y	4 nM	119 ± 22	24,651	~10 μM	99 ± 41	23,866	3 μM	32 ± 13	7552
H305F;H397Y;C410Y	C.A.	<5	9529	C.A.	<5	11,134	C.A.	<5	8448

EC_{50} values were calculated using GraphPad Prism and a non-linear regression extrapolation. Fold activations were calculated by dividing the highest level of activation by the lowest level of activation in triplicate experiments. C.A. indicates constitutive activity.

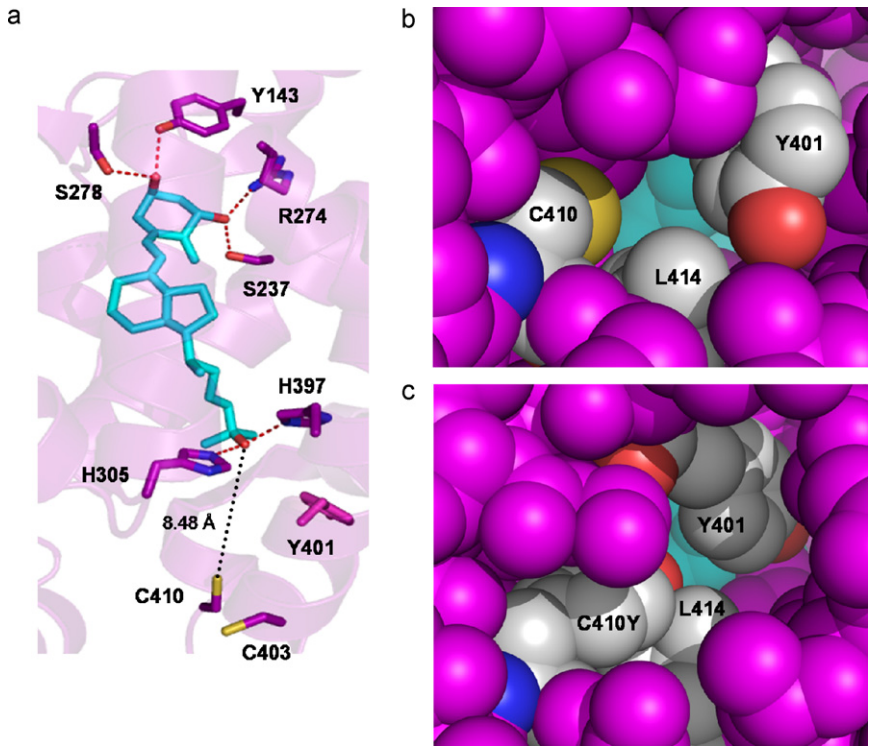

Fig. 4. (a) Cysteine 410 does not make direct contacts with the natural ligand (pdb: 1DB1). Hydrogen bonds and distance measured represented by (- - -) and (· · ·), respectively. *In silico* docking of (b) wthVDR and (c) hVDRC410Y with Cholecalciferol. Ligand and hVDR residues shown in cyan and magenta, respectively. The increase in bulk with C410Y and the repositioning of neighboring residues (e.g. Y401) contributes to the filling of a cavity at that end of the pocket.

variants with various ligands would not necessarily be expected due to the location of the residue in the LBD. However, in looking at the hVDR crystal structure, the presence of a cavity at the end of the pocket containing residues H305, H397, Y401 and C410 was observed. *In silico* docking of the wild-type hVDR and C410Y variant with cholecalciferol using Auto-dock Vina, suggests that the increase in bulk at the C410 position contributes to the filling of this cavity and possibly leading to the molecular interactions necessary for the enhanced and novel activation observed with LCA and chole, respectively (Fig. 4b and c) [50].

When tested in liquid quantitation assays of chemical complementation with 1α, 25(OH)$_2$D$_3$, LCA and chole in histidine selective media (SC-HLW with 0.1 mM 3-AT), most of the C410 variants behaved similar to the wild-type hVDR (Fig. 5a–c). More specifically, with 1α, 25(OH)$_2$D$_3$ ligand activated growth was observed for C410F, C410A, C410S, C410N, C410H, C410L, C410M, C410T, and C410K at 10 nM with an ~EC$_{50}$ > 10 nM, as shown in Fig. 5a, indicating a wide range of tolerance at this position for different types of residues. Ligand activated growth was not observed with C410W, which could imply that excessive bulk is not tolerated at this position (Fig. 5a). Overall, position C410 is fairly tolerant of mutations with the variants studied displaying profiles similar to that of the wild-type receptor (and C410Y) but with a 10-fold decrease in sensitivity when tested with 1α, 25(OH)$_2$D$_3$.

When tested with LCA, similar to the C410Y variant, C410F exhibited ligand activated growth at 100 nM with an EC$_{50}$ = 54 nM (Fig. 5b). As shown in Fig. 5b, similar to the wild-type hVDR, ligand activated growth at 10 μM with an ~EC$_{50}$ > 10 μM was observed for the rest of the C410 variants. C410W, which did not show growth with the natural ligand, also displayed ligand activated growth with LCA at 10 μM (~EC$_{50}$ > 10 μM), indicating that the increase of bulk and packing of the cavity at this end of the pocket contributes to activation with LCA (Fig. 5b). When tested with chole, C410F once again exhibited a ligand activated growth profile similar to that of C410Y with growth at 10 μM and an ~EC$_{50}$ > 10 μM (Fig. 5c). Like the wild-type hVDR and as shown in Fig. 5c, the rest of the C410 variants (including C410W) did not display ligand activated growth with chole.

3.5. Enhancing the sensitivity of variant hVDRC410Y further

Previously in our lab via random mutagenesis, a hVDR variant, hVDRH305F;H397Y, was engineered to activate in response to cholecalciferol [55]. Interestingly, both of the residues mutated in this variant and residue C410 are positioned on the same end of the hVDR's LBP, near the cavity previously mentioned (Fig. 4). To determine whether the effects of the H305F, H397Y and C410Y mutations on ligand activation would be additive, different combinations of these mutations were introduced into the hVDR. The resulting variants were tested in cell culture assays using HEK 293T cells with 1α, 25(OH)$_2$D$_3$, LCA and chole.

The variants H305F and C410Y showed EC$_{50}$ values of 4 nM and 1 nM with 1α, 25(OH)$_2$D$_3$, and ~10 μM and 3 μM with LCA, respectively. The variant H305F;C410Y displayed slightly higher sensitivity for 1α, 25(OH)$_2$D$_3$ and enhanced sensitivity for LCA (~10-fold compared to C410Y), compared to the other variants tested with an EC$_{50}$ < 1 nM and a 54-fold activation and an EC$_{50}$ = 0.3 μM and a 28-fold activation, respectively (Fig. 6a and b, and Table 1). With chole, the variants H305F and C410Y showed EC$_{50}$ values of 2 μM and 4 μM, respectively. H305F;H397Y and H305F;C410Y shared the same enhanced sensitivity for chole (~10-fold compared to C410Y), with an EC$_{50}$ = 0.3 μM and a 42-fold activation and an EC$_{50}$ = 0.2 μM and a 14-fold activation, respectively (Fig. 6c and Table 1). Interestingly, the variant H305F;H397Y;C410Y displayed constitutive activity, indicating that the receptor is in an active conformation, with activation observed in the absence of an exogenous small molecule ligand (Fig. 6a–c).

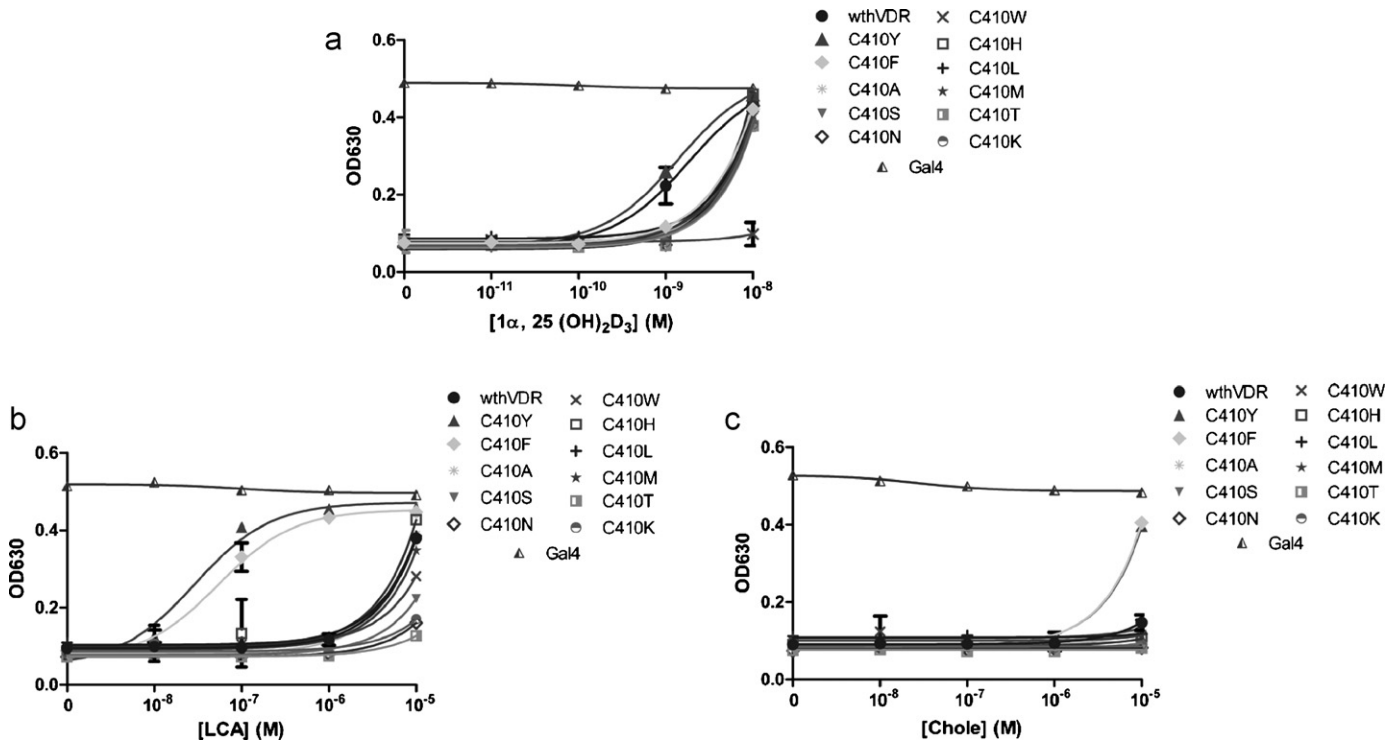

Fig. 5. Mutational tolerance of residue C410 in the hVDR: variant hVDRC410F behaves like hVDRC410Y. Quantitation assays of wthVDR and hVDRC410 variants in histidine selective media with (a) 1α, 25(OH)$_2$D$_3$. Ligand activated growth is observed for wild-type hVDR and C410Y at 1 nM. Ligand activated growth is observed for C410 F, A, S, N, H, L, M, T, and K at 10 nM. Growth is not observed for C410W. (b) LCA. Ligand activated growth is observed for wild-type hVDR and most hVDRC410 variants at 10 μM. Ligand activated growth is observed for C410Y and F at 100 nM. (c) chole. Ligand activated growth is observed for C410Y and F at 10 μM. Gal4 is a ligand independent transcription factor and was used as a positive control. Optical density readings were taken at a wavelength of 630 nm (OD630), measuring cell growth based on turbidity.

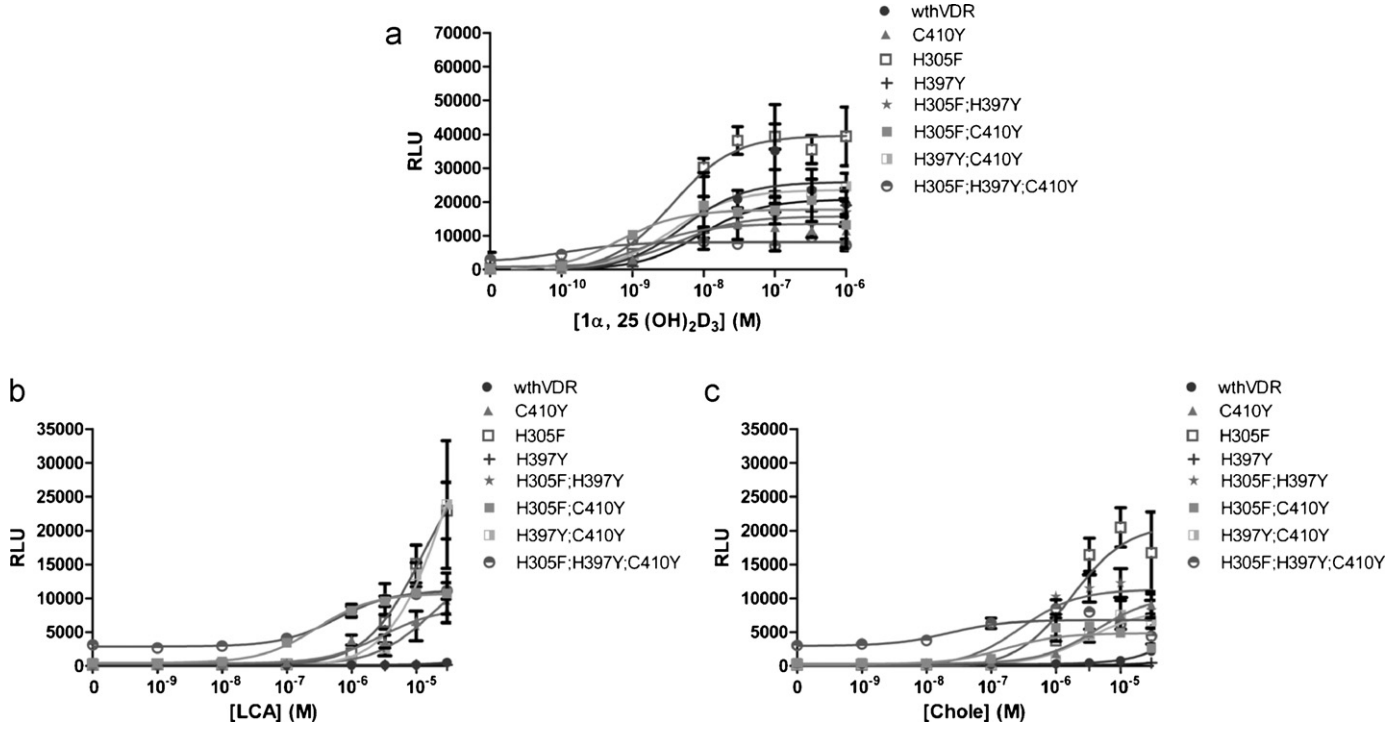

Fig. 6. Enhancing the sensitivity of variant hVDRC410Y further: activity of wthVDR and hVDR variants in mammalian cell culture assays using HEK 293T cells with (a) 1α, 25(OH)$_2$D$_3$ (b) LCA and (c) chole. Variant hVDRH305F;C410Y displays slightly higher sensitivity for 1α, 25(OH)$_2$D$_3$ and enhanced sensitivity for LCA, compared to the rest of the hVDR constructs tested. hVDRH305F;H397Y and hVDRH305F;C410Y share the same enhanced sensitivity for chole. Activity was measured in relative light units (RLU) derived from the measurement of luciferase activity and normalized against β-galactosidase activity. See Table 1 for EC$_{50}$, fold activation and maximum activation values.

4. Discussion

Due to their role as transcription factors, of regulating genes involved in all physiological activities upon ligand binding, understanding the general structural features of nuclear receptors is essential. However, equally as important is gaining knowledge of specific molecular interactions that occur between a receptor and its ligand(s), as they contribute towards the activation or repression of target genes. In the case of the human vitamin D receptor (hVDR), insight into the role and tolerance of specific residues within the receptor's ligand binding pocket (LBP) helps elucidate structural and functional parameters of the receptor and its ligands. For example, the crystal structure of hVDRH305Q (bound to the natural ligand), a variant associated with hereditary vitamin D-resistant rickets (HVDRR) was recently solved, providing insight on how the protein adopts the active conformation despite the structural effects of the H305Q mutation, as well as serving as the basis for the rational design of ligands for the treatment of HVDRR [63]. To date, mutational assessments of the hVDR have focused on alanine scanning and residues typically lining the LBP and that are involved in direct interactions with the ligand, such as hydrogen bonds. A comprehensive analysis of the tolerance of these residues in the binding and activation of the receptor by its ligands has not been performed. Furthermore, residues not in contact with the ligand or that do not line the LBP can also play an important role in determining the activation profiles observed for nuclear receptors, and therefore need to be explored further.

Previous hVDR structure–function analyses were used to rationally design a library of hVDR variants, in quest of exploring how chemical and physical changes within the LBP affect receptor–ligand interactions, thus receptor function. Cholecalciferol (chole), a precursor in the $1\alpha,25(OH)_2D_3$ biosynthetic pathway lacks two of the three hydroxyl groups present in 1α, $25(OH)_2D_3$, the receptor's natural ligand, and does not activate the wild-type receptor (Figs. 1a and 2c). This small molecule was chosen as the target ligand for engineering of the hVDR, as binding and activation of a variant could indeed provide insight into the molecular interactions necessary and/or that contribute to unique activation profiles.

Despite the fact that a hVDR library was designed to assess the mutational tolerance of two residues in helix 11, H397 and Y401, a variant C410Y, which displayed a 100-fold increase in sensitivity towards lithocholic acid (LCA) in comparison to the wild-type hVDR (EC_{50} = 29 nM) was discovered using chemical complementation in yeast (Fig. 2c). This variant was also activated by chole with an $\sim EC_{50} > 10\ \mu M$, whereas the wild-type hVDR is not (Fig. 2c). The presence of a tyrosine at the C410 position resulting in enhanced activity with LCA and novel activation with chole led to interest in determining whether a physical or chemical property of the residue was responsible for these activation profiles; in this case increased bulkiness and hydrogen bonding capability were to be considered.

When residue C410 was further assessed for its tolerance to varying amino acids and tested with the natural ligand, 1α, $25(OH)_2D_3$, most of the C410 variants (F, A, S, N, H, L, M, T, and K) showed a 10-fold decrease in sensitivity compared to the wild-type hVDR and C410Y variant (Fig. 5a). Despite residue C410's distance from 1α, $25(OH)_2D_3$, the fact that this position tolerated a wide range of amino acids including alanine was surprising, indicating that perhaps this residue does not contribute to the activation of the hVDR by its natural ligand; as seen with the rat VDR (rVDR) where the presence of an asparagine at this position results in comparable activation with 1α, $25(OH)_2D_3$. However, there seems to be some limitation to this tolerance, as observed with C410W, which did not display any growth (Fig. 5a). Tryptophan has the largest volume among all amino acids, 227.8 $Å^3$, and the significantly increased bulkiness at the C410 position may disrupt residue packing within the LBD [64].

Despite the fact that with 1α, $25(OH)_2D_3$ a range of tolerance is observed at the C410 position, the same trend does not seem to be observed with other ligands. As a matter of fact, the C410 residue along with C403, has been implicated to be involved in mediating opposing effects in two species of the VDR (e.g. the antagonistic effect of TEI-9647 on the hVDR vs. the agonistic effect of TEI-9647 on the rVDR) [65–67]. Recent crystal structures and MALDI-TOF MS studies of various hVDR/rVDR complexes with TEI-9647 provided insight on the structural mechanism underlying these species-specific effects [68]. Interestingly, as shown in this work, the presence of a tyrosine at the C410 position results in a novel activation profile with both LCA and chole in comparison to the wild-type hVDR. In addition to the tyrosine, the same activation profiles are observed with C410F, emphasizing the importance of bulkiness for activation with both ligands, as well as suggesting that the presence of a hydrogen bonding residue versus a hydrophobic one at C410 does not seem to affect the overall activity obtained with these ligands (Fig. 5b and c). Both LCA and chole have reduced molecular volumes compared to the natural ligand, $1\alpha,25(OH)_2D_3$. As a result, the increased bulkiness at the C410 position (volumes: cysteine 108.5 $Å^3$, phenylalanine 189.9 $Å^3$ and tyrosine 193.6 $Å^3$) may contribute additional contacts by decreasing the overall volume of the hVDR's LBP, and filling the cavity present at that end of the pocket as suggested by *in silico* docking results (Fig. 4b and c) [64]. However, as shown by the H305F;H397Y;C410Y variant, a drastic decrease in the volume of the LBP can result in constitutive activity, potentially due to an 'over-stabilized' active conformation and/or significantly enhanced hVDR–coactivator interactions (Fig. 6a–c).

Overall, this work seems to support the VDR ensemble model over the conventional two-state, induced-fit model. In the ensemble model apo-VDR exists in multiple conformations and contains two distinct but overlapping ligand binding pockets, and the varying activation profiles such as those observed in this work for different ligands are likely a result of shifts in the distribution of these VDR conformations [69–72]. Additionally, the VDR ensemble model proposes that helix 12 can exist in a closed, *holo*-like orientation in the absence of ligand suggesting the possibility of a constitutively active VDR construct to be engineered, as was observed in this work with the H305F;H397Y;C410Y variant.

Overall, a better understanding of the structural and functional relationships between the human vitamin D receptor (hVDR) and its ligands was achieved. A variant with a mutated residue (C410) that does not line the receptor's ligand binding pocket (LBP) and as a result does not make direct contacts with the natural ligand, was observed to display enhanced activation with a known hVDR ligand (lithocholic acid) as well as activation with a novel small molecule (cholecalciferol). When combined with an additional mutation on the same end of the LBP, H305F, the receptor's sensitivity for these ligands was enhanced further, emphasizing the importance of bulkiness at this end of the pocket for activation with both ligands. Previous work on the hVDR has focused on residues lining the receptor's LBP; however the effects of mutating residue C410 not only serve as an example of the significant impact distant residues can have on receptor activation with different ligands but also emphasize the important role physical properties of residues, such as volume, can play for specific ends of the LBP compared to chemical properties. Future work investigating the effects of C410Y on ligand binding and coactivator interactions would provide additional insight into the ligand-specific effects of this mutation on the activity profiles of the hVDR.

Acknowledgements

The authors would like to thank several colleagues for their contributions to this work. In particular, thanks to Dr. Loren Williams (Georgia Tech) for sharing his modeling expertise and Jennifer Taylor for mammalian cell culture training. We are grateful to Sanaz Jalalat, Lena James, and Eric Anderson for help with experimental set-ups. This work was supported by the National Institutes of Health (Grant # 1R01GM075832).

Appendix A. Supplementary data

Supplementary data associated with this article can be found, in the online version, at doi:10.1016/j.jsbmb.2011.08.003.

References

[1] D.J. Mangelsdorf, C. Thummel, M. Beato, P. Herrlich, G. Schutz, K. Umesono, B. Blumberg, P. Kastner, M. Mark, P. Chambon, R.M. Evans, The nuclear receptor superfamily-the 2nd decade, Cell 83 (6) (1995) 835–839.
[2] M. Robinson-Rechavi, A.S. Carpentier, M. Duffraisse, V. Laudet, How many nuclear hormone receptors are there in the human genome? Trends Genet. 17 (10) (2001) 554–556.
[3] V. Laudet, H. Gronemeyer, The Nuclear Receptor FactsBook, Academic Press, London, 2002.
[4] L. Nagy, J.W.R. Schwabe, Mechanism of the nuclear receptor molecular switch, Trends Biochem. Sci. 29 (6) (2004) 317–324.
[5] P. Chambon, The nuclear receptor superfamily: a personal retrospect on the first two decades, Mol. Endocrinol. 19 (6) (2005) 1418–1428.
[6] R.M. Evans, The nuclear receptor superfamily: a Rosetta stone for physiology, Mol. Endocrinol. 19 (6) (2005) 1429–1438.
[7] P. Germain, B. Staels, C. Dacquet, M. Spedding, V. Laudet, Overview of nomenclature of nuclear receptors, Pharmacol. Rev. 58 (4) (2006) 685–704.
[8] H. Gronemeyer, J.A. Gustafsson, V. Laudet, Principles for modulation of the nuclear receptor superfamily, Nat. Rev. Drug Discov. 3 (11) (2004) 950–964.
[9] K. Jepsen, M.G. Rosenfeld, Biological roles and mechanistic actions of co-repressor complexes, J. Cell Sci. 115 (4) (2002) 689–698.
[10] Y. Li, M.H. Lambert, H.E. Xu, Activation of nuclear receptors: a perspective from structural genomics, Structure 11 (7) (2003) 741–746.
[11] N.J. McKenna, B.W. O'Malley, Minireview: Nuclear receptor coactivators—an update, Endocrinology 143 (7) (2002) 2461–2465.
[12] N.J. McKenna, J.M. Xu, Z. Nawaz, S.Y. Tsai, M.J. Tsai, B.W. O'Malley, Nuclear receptor coactivators: multiple enzymes, multiple complexes, multiple functions, J. Steroid Biochem. Mol. Biol. 69 (1–6) (1999) 3–12.
[13] O. Wrange, J.A. Gustafsson, Separation of the hormone-binding and DNA-binding sites of the hepatic glucocorticoid receptor by means of proteolysis, J. Biol. Chem. 253 (3) (1978) 856–865.
[14] A. Klug, J.W.R. Schwabe, Zinc fingers, FASEB J. 9 (8) (1995) 597–604.
[15] J.M. Berg, DNA-binding specificity of steroid-receptors, Cell 57 (7) (1989) 1065–1068.
[16] J.M. Wurtz, W. Bourguet, J.P. Renaud, V. Vivat, P. Chambon, D. Moras, H. Gronemeyer, A canonical structure for the ligand-binding domain of nuclear receptors, Nat. Struct. Biol. 3 (1) (1996) 87–94.
[17] D. Moras, H. Gronemeyer, The nuclear receptor ligand-binding domain: structure and function, Curr. Opin. Cell Biol. 10 (3) (1998) 384–391.
[18] D.M. Lonard, B.W. O'Malley, Nuclear receptor coregulators: judges, juries, and executioners of cellular regulation, Mol. Cell 27 (5) (2007) 691–700.
[19] W. Bourguet, P. Germain, H. Gronemeyer, Nuclear receptor ligand-binding domains: three-dimensional structures, molecular interactions and pharmacological implications, Trends Pharmacol. Sci. 21 (10) (2000) 381–388.
[20] N.J. McKenna, R.B. Lanz, B.W. O'Malley, Nuclear receptor coregulators: cellular and molecular biology, Endocr. Rev. 20 (3) (1999) 321–344.
[21] N.J. McKenna, B.W. O'Malley, Combinatorial control of gene expression by nuclear receptors and coregulators, Cell 108 (4) (2002) 465–474.
[22] M.R. Haussler, G.K. Whitfield, C.A. Haussler, J.C. Hsieh, P.D. Thompson, S.H. Selznick, C.E. Dominguez, P.W. Jurutka, The nuclear vitamin D receptor: biological and molecular regulatory properties revealed, J. Bone Miner. Res. 13 (3) (1998) 325–349.
[23] G.N. Hendy, K.A. Hruska, S. Mathew, D. Goltzman, New insights into mineral and skeletal regulation by active forms of vitamin D, Kidney Int. 69 (2) (2006) 218–223.
[24] R. Bouillon, W.H. Okamura, A.W. Norman, Structure–function-relationships in the vitamin-D endocrine system, Endocr. Rev. 16 (2) (1995) 200–257.
[25] M.R. Haussler, C.A. Haussler, P.W. Jurutka, P.D. Thompson, J.C. Hsieh, L.S. Remus, S.H. Selznick, G.K. Whitfield, The vitamin D hormone and its nuclear receptor: molecular actions and disease states, J. Endocrinol. 154 (1997) S57–S73.
[26] N. Rochel, J.M. Wurtz, A. Mitschler, B. Klaholz, D. Moras, The crystal structure of the nuclear receptor for vitamin D bound to its natural ligand, Mol. Cell 5 (1) (2000) 173–179.
[27] P.J. Malloy, J.W. Pike, D. Feldman, The vitamin D receptor and the syndrome of hereditary 1,25-dihydroxyvitamin D-resistant rickets, Endocr. Rev. 20 (2) (1999) 156–188.
[28] M. Makishima, T.T. Lu, W. Xie, G.K. Whitfield, H. Domoto, R.M. Evans, M.R. Haussler, D.J. Mangelsdorf, Vitamin D receptor as an intestinal bile acid sensor, Science 296 (5571) (2002) 1313–1316.
[29] K. Yamamoto, M. Choi, D. Abe, M. Shimizu, S. Yamada, Alanine scanning mutational analysis of the ligand binding pocket of the human Vitamin D receptor, J. Steroid Biochem. Mol. Biol. 103 (3–5) (2007) 282–285.
[30] M. Choi, K. Yamamoto, T. Itoh, M. Makishima, D.J. Mangelsdorf, D. Moras, H.F. DeLuca, S. Yamada, Interaction between vitamin D receptor and vitamin D ligands: two-dimensional alanine scanning mutational analysis, Chem. Biol. 10 (3) (2003) 261–270.
[31] S. Yamada, K. Yamamoto, Ligand recognition by vitamin D receptor: Total alanine scanning mutational analysis of the residues lining the ligand binding pocket of vitamin D receptor, Curr. Top. Med. Chem. 6 (12) (2006) 1255–1265.
[32] K. Yamamoto, D. Abe, N. Yoshimoto, M. Choi, K. Yamagishi, H. Tokiwa, M. Shimizu, M. Makishima, S. Yamada, Vitamin D receptor: ligand recognition and allosteric network, J. Med. Chem. 49 (4) (2006) 1313–1324.
[33] M.W. Choi, K. Yamamoto, H. Masuno, K. Nakashima, T. Taga, S. Yamada, Ligand recognition by the vitamin D receptor, Bioorg. Med. Chem. 9 (7) (2001) 1721–1730.
[34] M.D. Reddy, L. Stoynova, A. Acevedo, E.D. Collins, Residues of the human nuclear vitamin D receptor that form hydrogen bonding interactions with the three hydroxyl groups of 1alpha,25-dihydroxyvitamin D3, J. Steroid Biochem. Mol. Biol. 103 (3–5) (2007) 347–351.
[35] F. Molnar, R. Sigueiro, Y. Sato, C. Araujo, I. Schuster, P. Antony, J. Peluso, C. Muller, A. Mourino, D. Moras, N. Rochel, 1 alpha, 25(OH)(2)-3-Epi-Vitamin D-3, a natural physiological metabolite of vitamin D-3: its synthesis, biological activity and crystal structure with its receptor, Plos One 6 (3) (2011).
[36] C. Carlberg, Molecular basis of the selective activity of vitamin D analogues, J. Cell. Biochem. 88 (2) (2003) 274–281.
[37] C. Carlberg, F. Molnar, Detailed molecular understanding of agonistic and antagonistic vitamin D receptor ligands, Curr. Top. Med. Chem. 6 (12) (2006) 1243–1253.
[38] R. Adachi, A.I. Shulman, K. Yamamoto, I. Shimomura, S. Yamada, D.J. Mangelsdorf, M. Makishima, Structural determinants for vitamin D receptor response to endocrine and xenobiotic signals, Mol. Endocrinol. 18 (1) (2004) 43–52.
[39] F. Molnar, M. Perakyla, C. Carlberg, Vitamin D receptor agonists specifically modulate the volume of the ligand-binding pocket, J. Biol. Chem. 281 (15) (2006) 10516–10526.
[40] K. Yamagishi, H. Tokiwa, M. Makishima, S. Yamada, Interactions between 1 alpha, 25(OH)(2)D-3 and residues in the ligand-binding pocket of the vitamin D receptor: a correlated fragment molecular orbital study, J. Steroid Biochem. Mol. Biol. 121 (1–2) (2010) 63–67.
[41] G. Chiellini, H.F. DeLuca, The importance of stereochemistry on the actions of vitamin D, Curr. Top. Med. Chem. 11 (7) (2011) 840–859.
[42] R. Higuchi, B. Krummel, R.K. Saiki, A general-method of invitro preparation and specific mutagenesis of DNA fragments—study of protein and DNA interactions, Nucleic Acids Res. 16 (15) (1988) 7351–7367.
[43] R.D. Gietz, R.A. Woods, Transformation of Yeast by Lithium Acetate/Single-stranded Carrier DNA/Polyethylene Glycol Method, Guide to Yeast Genetics and Molecular and Cell Biology, Pt B, Academic Press Inc., San Diego, 2002, pp. 87–96.
[44] J.L. Taylor, P. Rohatgi, H.T. Spencer, D.F. Doyle, B. Azizi, Characterization of a molecular switch system that regulates gene expression in mammalian cells through a small molecule, BMC Biotechnol. 10 (2010) 15.
[45] A. Sali, T.L. Blundell, Comparative protein modeling by satisfaction of spatial restraints, J. Mol. Biol. 234 (3) (1993) 779–815.
[46] J. Damborsky, M. Prokop, J. Koca, TRITON: graphic software for rational engineering of enzymes, Trends Biochem. Sci. 26 (1) (2001) 71–73.
[47] H.M. Berman, J. Westbrook, Z. Feng, G. Gilliland, T.N. Bhat, H. Weissig, I.N. Shindyalov, P.E. Bourne, The protein data bank, Nucleic Acids Res. 28 (1) (2000) 235–242.
[48] E.F. Pettersen, T.D. Goddard, C.C. Huang, G.S. Couch, D.M. Greenblatt, E.C. Meng, T.E. Ferrin, UCSF chimera—a visualization system for exploratory research and analysis, J. Comput. Chem. 25 (13) (2004) 1605–1612.
[49] M.F. Sanner, Python: a programming language for software integration and development, J. Mol. Graph. Modell. 17 (1) (1999) 57–61.
[50] O. Trott, A.J. Olson, AutoDock Vina: improving the speed and accuracy of docking with a new scoring function, efficient optimization, and multithreading, J. Comput. Chem. (2009).
[51] B. Azizi, E.I. Chang, D.F. Doyle, Chemical complementation: small-molecule-based genetic selection in yeast, Biochem. Biophys. Res. Commun. 306 (3) (2003) 774–780.
[52] L.J. Schwimmer, P. Rohatgi, B. Azizi, K.L. Seley, D.F. Doyle, Creation and discovery of ligand–receptor pairs for transcriptional control with small molecules, Proc. Natl. Acad. Sci. U.S.A. 101 (41) (2004) 14707–14712.
[53] K. Baker, C. Bleczinski, H.N. Lin, G. Salazar-Jimenez, D. Sengupta, S. Krane, V.W. Cornish, Chemical complementation: a reaction-independent genetic assay for enzyme catalysis, Proc. Natl. Acad. Sci. U.S.A. 99 (26) (2002) 16537–16542.
[54] B.L. Drees, Progress and variations in two-hybrid and three-hybrid technologies, Curr. Opin. Chem. Biol. 3 (1) (1999) 64–70.
[55] A.M. Ousley, H.S. Castillo, A. Duraj-Thatte, D.F. Doyle, B. Azizi, A human vitamin D receptor mutant activated by cholecalciferol, J. Steroid Biochem. Mol. Biol. 125 (3–5) (2011) 202–210.

[56] P. James, J. Halladay, E.A. Craig, Genomic libraries and a host strain designed for highly efficient two-hybrid selection in yeast, Genetics 144 (4) (1996) 1425–1436.
[57] A.R. Gillies, G. Skretas, D.W. Wood, Engineered systems for detection and discovery of nuclear hormone-like compounds, Biotechnol. Prog. 24 (2008) 8–16.
[58] K. Struhl, R.W. Davis, Production of a functional eukaryotic enzyme in escherichia-coli—cloning and expression of yeast structural gene for imidazoleglycerolphosphate dehydratase (HIS3), Proc. Natl. Acad. Sci. U.S.A. 74 (12) (1977) 5255–5259.
[59] R. Adachi, Y. Honma, H. Masuno, K. Kawana, L. Shimomura, S. Yamada, M. Makishima, Selective activation of vitamin D receptor by lithocholic acid acetate, a bile acid derivative, J. Lipid Res. 46 (1) (2005) 46–57.
[60] M.F. Boehm, P. Fitzgerald, A.H. Zou, M.G. Elgort, E.D. Bischoff, L. Mere, D.E. Mais, R.P. Bissonnette, R.A. Heyman, A.M. Nadzan, M. Reichman, E.A. Allegretto, Novel nonsecosteroidal vitamin D mimics exert VDR-modulating activities with less calcium mobilization than 1,25-dihydroxyvitamin D-3, Chem. Biol. 6 (5) (1999) 265–275.
[61] W. Humphrey, A. Dalke, K. Schulten, VMD: visual molecular dynamics, J. Mol. Graph. 14 (1) (1996) 33–38.
[62] R.E. Watkins, G.B. Wisely, L.B. Moore, J.L. Collins, M.H. Lambert, S.P. Williams, T.M. Willson, S.A. Kliewer, M.R. Redinbo, The human nuclear xenobiotic receptor PXR: structural determinants of directed promiscuity, Science 292 (5525) (2001) 2329–2333.
[63] N. Rochel, S. Hourai, D. Moras, Crystal structure of hereditary vitamin D-resistant rickets—associated mutant H305Q of vitamin D nuclear receptor bound to its natural ligand, J. Steroid Biochem. Mol. Biol. 121 (1–2) (2010) 84–87.
[64] J. Reichert, J. Suhnel, The IMB Jena Image Library of Biological Macromolecules: 2002 update, Nucleic Acids Res. 30 (1) (2002) 253–254.
[65] E. Ochiai, D. Miura, H. Eguchi, S. Ohara, K. Takenouchi, Y. Azuma, T. Kamimura, A.W. Norman, S. Ishizuka, Molecular mechanism of the vitamin D antagonistic actions of (23S)-25-dehydro-1 alpha-hydroxyvitamin D-3-26, 23-lactone depends on the primary structure of the carboxyl-terminal region of the vitamin D receptor, Mol. Endocrinol. 19 (5) (2005) 1147–1157.
[66] M. Perakyla, F. Molnar, C. Carlberg, A structural basis for the species-specific antagonism of 26, 23-lactones on vitamin D signaling, Chem. Biol. 11 (8) (2004) 1147–1156.
[67] M.T. Mizwicki, C.M. Bula, P. Mahinthichaichan, H.L. Henry, S. Ishizuka, A.W. Norman, On the mechanism underlying (23S)-25-dehydro-1alpha(OH)-vitamin D3-26, 23-lactone antagonism of hVDRwt gene activation and its switch to a superagonist, J. Biol. Chem. 284 (52) (2009) 36292–36301.
[68] S. Kakuda, S. Ishizuka, H. Eguchi, M.T. Mizwicki, A.W. Norman, M. Takimoto-Kamimura, Structural basis of the histidine-mediated vitamin D receptor agonistic and antagonistic mechanisms of (23S)-25-dehydro-1 alpha-hydroxyvitamin D-3-26, 23-lactone, Acta Crystallogr. D Biol. Crystallogr. 66 (2010) 918–926.
[69] A.W. Norman, M.T. Mizwicki, D.P.G. Norman, Steroid-hormone rapid actions, membrane receptors and a conformational ensemble model, Nat. Rev. Drug Discov. 3 (1) (2004) 27–41.
[70] M.T. Mizwicki, D. Keidel, C.M. Bula, J.E. Bishop, L.P. Zanello, J.M. Wurtz, D. Moras, A.W. Norman, Identification of an alternative ligand-binding pocket in the nuclear vitamin D receptor and its functional importance in 1 alpha, 25(OH)(2)-vitamin D-3 signaling, Proc. Natl. Acad. Sci. U.S.A. 101 (35) (2004) 12876–12881.
[71] M.T. Mizwicki, A.W. Norman, The vitamin D sterol–vitamin D receptor ensemble model offers unique insights into both genomic and rapid-response signaling, Sci. Signal. 2 (75) (2009) re4.
[72] M.T. Mizwicki, D. Menegaz, S. Yaghmaei, H.L. Henry, A.W. Norman, A molecular description of ligand binding to the two overlapping binding pockets of the nuclear vitamin D receptor (VDR): structure–function implications, J. Steroid Biochem. Mol. Biol. 121 (1–2) (2010) 98–105.